LOCAL HEAT TRANSFER IN A STIRRED VESSEL WITH AND WITHOUT AERATION

WEI-MING LU,* CHIH-MING LAN, AND HSU-WEI FANG
Department of Chemical Enginnering, National Taiwan University
Taipei, Taiwan, R. O. C.

Keywords: Heat Transfer, Stirred Vessels, Thermister Probe, Aeration, Baffle Coil.

A positive temperature coefficient thermister is devised as a thermal probe to determine local heat transfer coefficients in a stirred vessel with a standard Rushton turbine impeller. The effects of aeration and flow patterns on the value of local heat transfer coefficients are discussed. Under most operating conditions, the highest flux is found at the impeller discharge region and the front side of the baffle plates. The mean Nusselt number for jacket and baffle type heat exchange elements is presented in terms of the modified Reynolds number and the other dimmensionless groups, as the results of the integration of the determind values of local heat transfer coefficients.

Introduction

Heat transfer in aerated stirred vessels is a very important operation in chemical and biological processes. Although there are numerous dimensionless correlations for the overall or integrated heat transfer coefficient for stirred vessels, the prediction of heat transfer for a given system is still quite complicated because the correlation are different from each other due to several factors, such as the geometry of the system, type and rotational speed of the impeller, fluid velocity and flow pattern of the fluid etc. In most large scale gas-liquid reactors, removal of heat from the reacting medium is usually achieved by internal heat transfer elements like spiral coil or baffle type heat exchange elements to acquire sufficient haet transfer area and also to save on the cost of structures.

In recent years, there have been only a few studies devoted to local process side heat transfer. Using an electrochemical technique, Man (1985) analogized the results of local variation of the mass transfer coefficient to heat transfer. Karcz and Strek (1985) used the same technique in an aerated stirred vessel with a dual turbine system. They pointed out in the impeller discharge region, heat transfer coefficients between liquid system and gas-liquid system has relation as:

$$\frac{h_{G-L}}{h_L} = \sqrt{\frac{f_{G-L}}{f_L}} \tag{1}$$

For dual impeller system, they proposed

$$\overline{Nu} = 0.419 \mathrm{Re}_{p,v}^{*\,0.22} \cdot Pr^{0.33} \left(\frac{\mu_w}{\mu_b}\right)^{-0.14} \tag{2}$$

Their results were 10~20% lower than those for a non-aerated system.

Using a micro foil sensor, Fasano *et al.* (1991) and Haam and Brodkey (1992) also determined local heat transfer coefficients for side wall and bottom surface. Instead of correlating the local heat transfer coefficient *Nu* as a function of power drawn by an impeller, they correlated *Nu* in terms of the dimensionless superficial velocity of gas.

Measurements of the local heat transfer coefficient are usually carried out by a thermal method or by analogy of mass transfer data. The conventional thermal method has the disadvantages of inaccuracy caused by heat loss to the surrounding area, and the difficuity of estimating the surface temperature accurately while the estimation by the analogy principle is limited due its complicate flow field.

To overcome these difficulties in determination of the local heat transfer coefficient, the Positive Temperature Coefficient Thermister (PTCT) was adopted in this study as a probe element to obtain local heat transfer rates in a stirred vessel with aeration. The effect of aeration on local heat transfer rate was examined as well as that of fluid flow.

1. Experimental

1.1 Thermister probe

Figure 1 shows a cross section drawing of the PTCT probe used in this study. The thermister element is a high temperature sintered product of barium titanate ($BaTiO_3$) and a trace amount of a rare earth element. The thermister element has the following merits which make it very suitable for a thermal probe to determind heat transfer coefficient:

(1) positive and large value of temperature coefficient of resistance,
(2) higher electrical resistance,
(3) applicable for high voltage,
(4) sensitive to heat and low specific heat.

Therefore, by applying electricity to the thermister elements under steady or pseudo steady state conditions, the temperature of the element can be easily controlled at an equilibrium temperature, which enables us to estimate

* Received on December 26, 1994. Correspondence concerning this article should be addressed to Wei-Ming Lu.

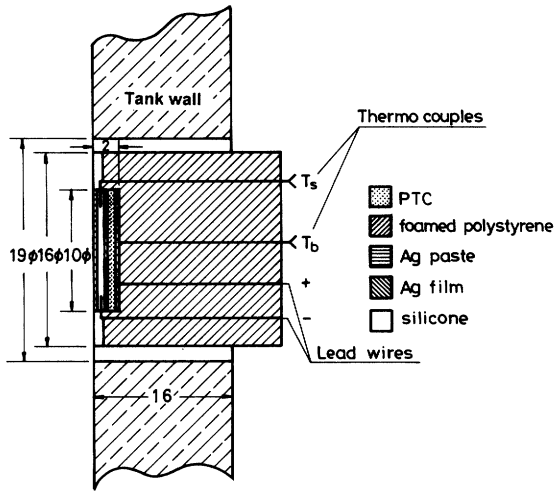

Fig. 1 Cross-sectional view of the thermister probe

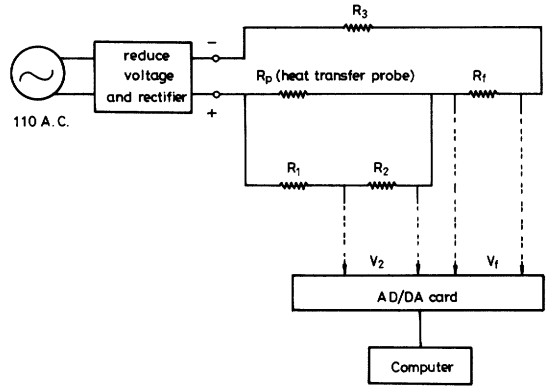

Fig. 2 Schematic of the circuit used measure local heat transfer coefficient

heat loss more accurately.

In the structure of the probe, foamed polystyrene was used as a support basis and as an insulator while the 2mm thick PTCT element was inlayed at the center of the surface. A thin silicon layer was applied on the surface of the element and surrounding area to avoid the dissipation of heat from the circumference and also for water proof. A hole of 19 mm diameter was drilled to insert the probe at each measure point. The probe was fixed firmly by use of silicone paste.

Figure 2 illustrates the circuit arrangement of the probe system, where R_1, R_2, R_3 and R_f are known reference resistances. This circuit design enables us to keep the voltage of electricity entering the AD/DA card below its limit. From Newton's law of convection, the heat flux from the probe surface can be given as

$$q_{conv} = hA(T_s - T_f), \tag{3}$$

and from the measured values of the current and voltages in the circuit, one has

$$I_p = V_f / R_f - V_2 / R_2 \tag{4}$$

and

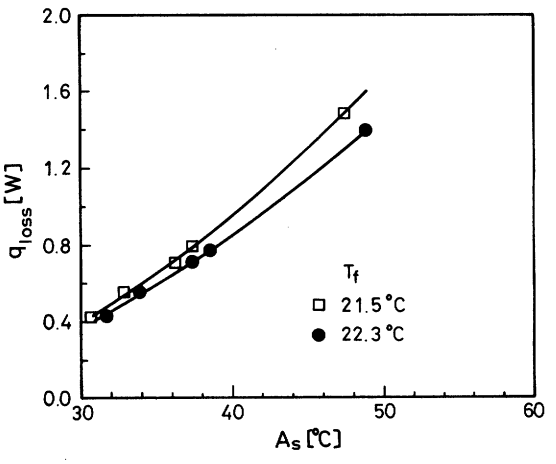

Fig. 3 Heat loss of the probe vs. T_s inder different fluid temperature T_f

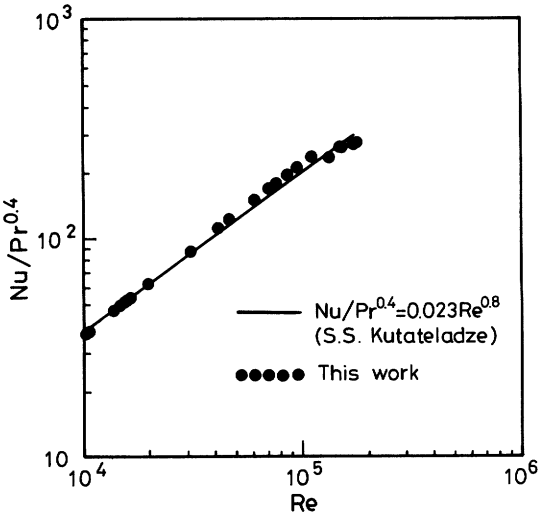

Fig. 4 Comparision of measured Local heat transfer coefficient in a pipe with Kutatelade's results

$$R_p = \frac{(V_2 / R_2)(R_1 + R_2)}{V_f / R_f - V_2 / R_2} \tag{5}$$

Since

$$q_{conv} = I_p^2 R_p - q_{loss} \tag{6}$$

substitutuon of Eq. (4) and Eq. (5) into this expression gives:

$$q_{conv} = \left(\frac{V_f}{R_f} - \frac{V_2}{R_2}\right)\left(\frac{V_2}{R_2}\right)(R_1 + R_2) - q_{loss} \tag{7}$$

Thus, if q_{loss} can be estimated correctly, the heat flux from the probe surface can be obtained from Eq. (7).

1.2 Estimation of heat loss from the probe

After placing a probe into a vessel containing a fluid (water), and applying electricity, soon the surface tempareture of the probe will reach an equilibrium value. From the conservation of energy, the heat generated by the probe can be given as:

$$I_p^2 R_p = q_{conv} + q_{loss} \tag{8}$$

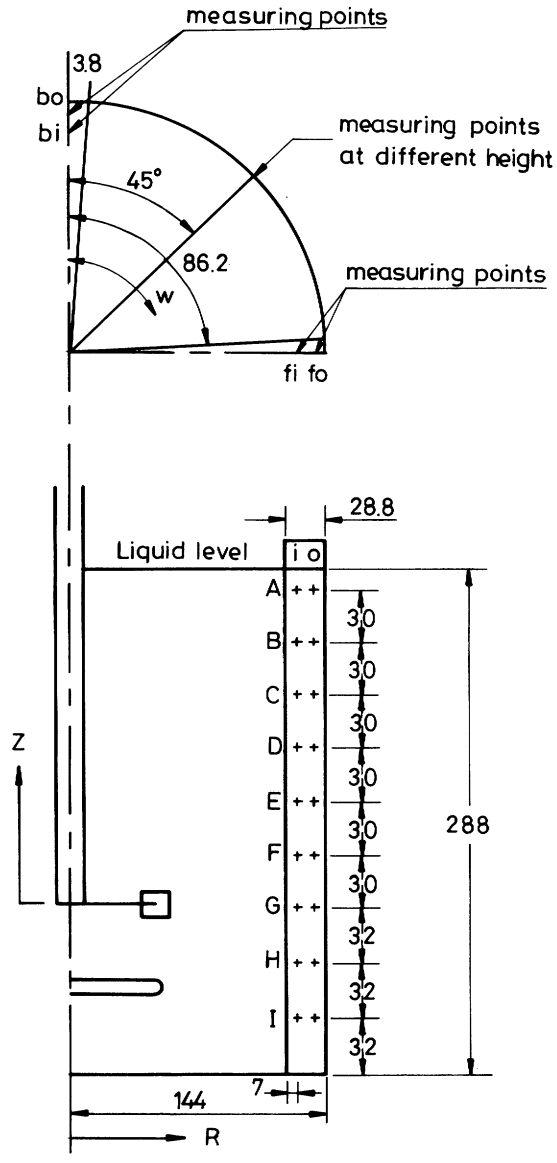

Fig. 5 Measurement positions for local heat transfer at the side wall of the vessel

Since heat loss to solid surrounding is not much affected by fluid velocity flowing through probe surface, q_{loss} is estimated by placing the probe vertically in a stagnant fluid, and h in Eq. (9) is calculated from the formula given by Churchill and Chu (1975).

Substitution of Eq. (3) into Eq. (8) gives:

$$q_{loss}(T_s, T_b, T_{f.....}) = q_{loss}(T_s, T_f) = I_p^2 R_p - hA(T_s - T_f) \quad (9)$$

In **Fig. 3**, the measured heat loss for various surface temperature are plotted for two different bulk fluid temperatures.

1.3 Testing the probe

In order assure the reliability of the PTCT Probe system, the device was used to measure heat transfer coefficients in a fluid flow system in a circular conduit under various flow velocities. As shown in **Fig. 4**, if Re is smaller than 10^5, the data determind by this device and the described method agree very well with Kutateladze's correlation (Kutateladze, 1957). Details of the method to determine the local heat transfer rate using a thermister probe can be found in Lan's thesis (Lan, 1993).

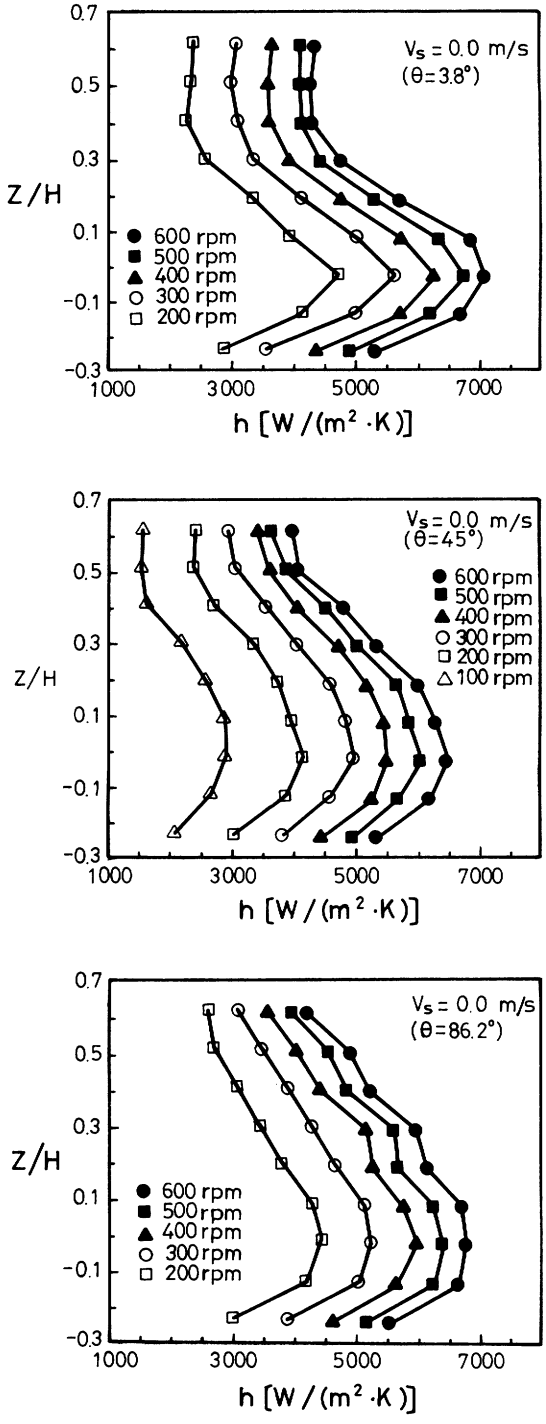

Fig. 6 Variation of local heat transfer coefficient with axial height under Vs = 0.0 m/s at different θ locations

1.4 The stirred tank

The investigation was carried out in a flat bottomed tank of the diameter T = 0.288m. A standard Rushton turbine ($T/3$) was installed 0.096m high from the bottom while air was supplied from a ring sparger of 0.092m diameter and having twelve holes of 0.001m diameter. Tap water and filtered air were used as the liquid and gas phases, respectively.

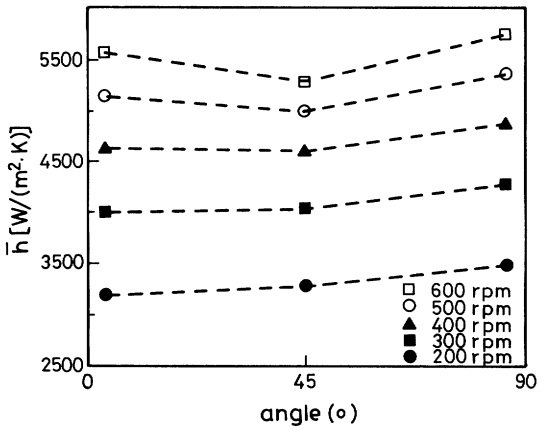

Fig. 7 Comparison of mean heat transfer coefficient at the different angles between the baffles under Vs = 0.0 m/s

Table 1 Local heat transfer coefficients at both sides of the baffle plates under non-aerated condtion (N = 6.67 rps)

Location	b_i	b_o	θ = 45° wall	f_i	f_o
Z/H = 0	6548.7	6514.0	5497.2	7055.8	6252.2
Z/H = 0.625	2692.7	3435.4	3498.6	4283.7	3229.5
average	4281.9	4647.7	4651.8	4959.8	4940.1

unit: [W/(m²·K)], Locations b_i, b_o, f_i and f_o as shown in Fig. 5

In order to examine the effect of the flow field on the rate of heat transfer in such an aerated stirred vessel, measurement points were located at different heights along both the tank wall (3.8°, 45° and 86.2°) and each side of the baffle plate as shown in **Fig. 5**. (In total 59 points were measured.)

2 Results and Discussion

2.1 Heat transfer coefficients in a stirred vessel under ungassed conditions

Figure 6a ~ 6c show how the value of local heat transfer coefficient varied with height and the speed of impeller rotation at three different θ locations under ungassed condition. Since the rate of heat transfer heavily depends on the velocity of the fluid sweeping along the surface, the highest value of the local heat transfer coefficient naturally was found at the impeller discharge region where fluid impinges on the wall at the maximum velocity. For a given θ location and operatiing conditions, the value of h had the maximum at Z/H = 0, and it decreased on both sides along the change in the height; however, the change of h along the height was different for each θ location. For the case of (θ = 86.2°), the change of h against axial height was more gentle while the decrease of h along the height at a location just behind the baffle (θ = 3.8°) was rather steeper and became almost flat as the height exceeded a distance of one diameter of the impeller (i. e. $Z/H \geq 0.3$).

This fact can be explained from difference in flow patterns in each location. At the location behind the

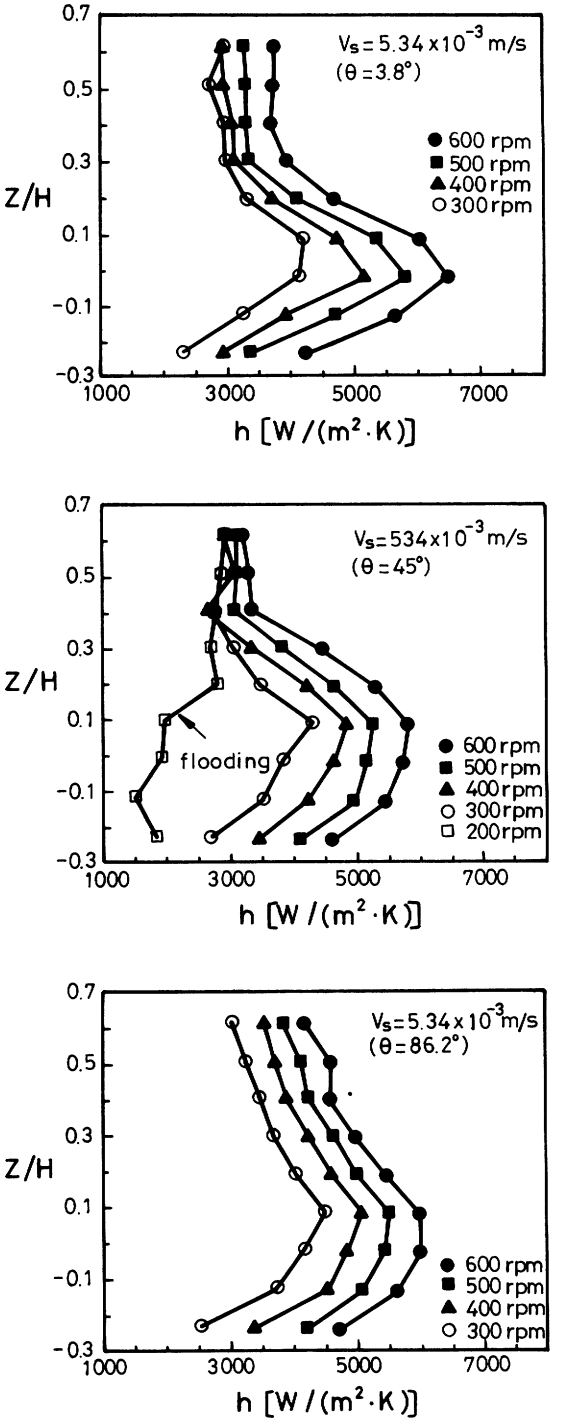

Fig. 8 Variation of local heat transfer coefficient with axial height under $Vs = 5.34 \times 10^{-3}$ m/s at different θ locations

baffle plate (θ = 3.8°), the flow shows a swirling or vortices type flow near the impeller discharge region (Ede, 1961), and the impeller characteristic had less effect on the upper zone of this location. It is interesting to examine the change of the values of h at this location under any operating conditions; the h measures at Z/H = 0 always had the highest value if it was compared with the value of h the other θ locations. This fact can be explained by the fact that the strong swirling flow can be seen at the discharge region of

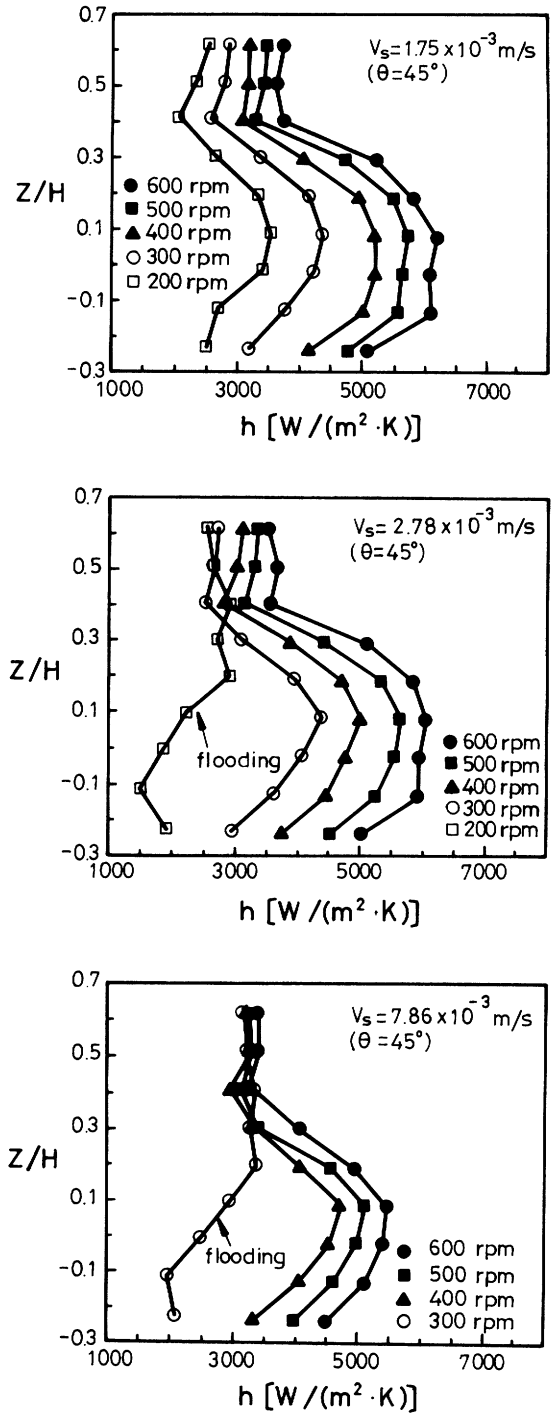

Fig. 9 Effect of gas flow rate on local heat transfer coefficient at $\theta = 45°$

the impeller at the location just behind the baffle plate, but the strenght of this swirling flow decays sharply along the increase in the height, which causes a steep decrease of h *vs.* Z/H and also results in a flat variation of in the upper region.

In **Fig. 7**, the mean value of heat transfer coefficients for nine different heights for these three different angle locations are shown for various rotational speeds. For a given rotational speed, the mean value of h at the plane in front of the baffle ($\theta = 86.2°$) is always the highest and the

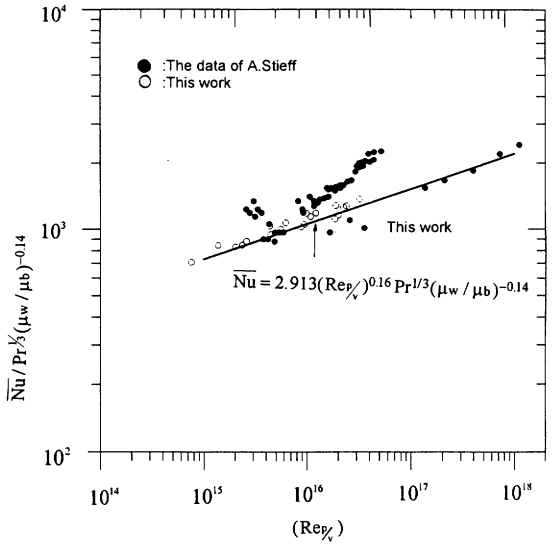

Fig. 10 Correlations of the mean heat transfer coefficient against the modified Reynolds number of the system

Table 2 Correlation of local heat transfer coefficients at both sides of baffle plates under aerated condtion

Position	Z/H	c	a
b_i	0	1.466	0.189
b_o	0	1.305	0.192
f_i	0	0.325	0.232
f_o	0	2.259	0.178
b_i	ave. of all Z/H	2.841	0.160
b_o	ave. of all Z/H	4.113	0.152
f_i	ave. of all Z/H	2.803	0.173
f_o	ave. of all Z/H	1.829	0.177

Locations b_i, b_o, f_i and f_o as shown in Fig. 5

difference between it and mean h at the 45° middle plane is approximately 5~7%, which is higher than 2% given by Bourne *et al.* (1985) for mass transfer rates. If the mean Nu at the 45° mid-plane can be correlated in the form of

$$\overline{Nu} = cRe^{a} \cdot Pr^{0.33}\left(\frac{\mu_w}{\mu_b}\right)^{-0.14} \tag{10}$$

it gives $a = 0.66$, $c = 0.729$,
i. e.

$$\overline{Nu} = 0.729Re^{0.66} \cdot Pr^{0.33}\left(\frac{\mu_w}{\mu_b}\right)^{-0.14}$$
$$\text{for} \quad 2.1\times 10^4 < Re < 1.1\times 10^5 \tag{11}$$

where $c = 0.729$ is taken after the existing correlation (Chiton, 1994) of $\overline{Nu}$ for jacket wall, which has $c = 0.74$. For all of the physical properties of fluid for calculation, the mean values of data at T_s and T_f are taken.

In **Table 1**, the variation of local heat transfer coefficients and the average values for both sides of the baffle plate are listed for two different heights. The values at the 45° mid-plane at the wall are also presented here for comparison. The front point near the impeller always has the highest local heat transfer coefficient and also the highest mean value. On the backside of the baffle plate, the value of local h at the impeller discharge region shows to

be quite high, but it becomes almost the lowest value in the region near the free surface. It is noticed that the average value of the mean heat transfer coefficient for the whole baffle has only approximately 10% higher than that obtained at the 45° mid-plane.

2.2 Heat transfer coefficients at various gas flow rates

In **Figures 8a ~ 8c**, how the value of h varies with height and rotational speeds for a considerable high gas flow rate of V_s = 0.00534 m/s (equivalent to 1.11VVM) at three different θ locations is shown. Since the location of maximum liquid velocity shifts upward due to aeration, the point of maximum h also shifts to the height Z/H = 0.1 except for the points behind the baffle (i. e. θ = 3.8°). The curves of θ = 3.8° and θ = 45° shown in Figure 8 show a flat variation of h at locations Z/H > 0.4 where the flow field in the upper region is not affected by the performance of the impeller while at the points in front of the baffle, h decays monotonously with the increase of height.

To examine how the gas flow rate will affect the values of local heat transfer coefficients, the plots of h vs. Z/H for several different gas flow rates are shown for the location θ = 45° in **Figures 9a ~ 9c** (also see Figure 7b). Before the status of gas dispersion in the system reaches flood stage, the trends of these plots are very similar to the results seen in the cases of ungassed conditions except for the shift of the highest h point from Z/H = 0 to Z/H = 0.1.

If the gas flow rate continuously increases, or the rotational speed of the impeller decreases to create a flooding situation, there occurs a sharp decrease in the value of h in the place near the impeller due to insufficient pumping of the impeller.

For a given rotational speed, no significant change in the upper region of the tank is observed because the flow of fluid in this region is not much affected by the pumping capability of impeller, but the up rising gas flow rates.

2.3 Correlation of $\overline{Nu}$ with dimensionless variables for aerated system

Loiseau and Charpentier (1977) indicated that Michel and Miller's experimental equation (Michel and Miller, 1962)

$$P_g = 0.83\left(\frac{P_0 N D^3}{Q_g^{0.56}}\right)^{0.46} \tag{12}$$

can be used to estimate the power drawn by a Rushton turbine impeller in its standard geometry, with a gas flow rate of 0.0005m/s ≤ V_s ≤ 0.09m/s and $1 < P_0ND^3/Q_g^{0.56} < 10^7$. For an ungassed system, Calderbank and Moo-Young (1961) educed from local isotropic turbulent and proposed that

$$Nu \propto Re_{p/v}^{1/4} Rr^{1/3} \tag{13}$$

to correlate the heat transfer coefficient with the power drawn by the impeller for a stirred vessel, where $Re_{p/v}$ is a modified Reynolds number and is defined as

$$Re_{p/v} = \frac{(P/V)T^4\rho^2}{\mu^3} \tag{14}$$

Modifying Eq. (13) by inserting $\left(\frac{\mu_w}{\mu_b}\right)^{-0.14}$ to include the effect of viscosity, Eq. (13) can be written in the form of

$$Nu = c \cdot (Re_{p/v})^a \cdot Pr^{\frac{1}{3}} \left(\frac{\mu_w}{\mu_b}\right)^{-0.14} \tag{15}$$

Since in most operations, the status of gas dispersion is either at loading or complete dispersion, which satisfies the condition $P_g >> P_a$ (aeration power) or $p/v \sim p_g/V$, it follows that

$$(Re_{p/v}) \approx (P_g/V) \cdot T^4 \cdot \rho^2 / \mu^3 \tag{16}$$

Figure 10 shows a plot of $\overline{Nu}$ at 45° mid-plane for air-water system, and they are compared with the data of Steiff *et al.* (1985). These results can be correlated as

$$\overline{Nu} = 2.913 Re_{p/v}^{0.16} \cdot Pr^{0.33} \left(\frac{\mu_w}{\mu_b}\right)^{-0.14} \tag{17}$$

for the range of $7.6*10^{14} < Re_{p/v} < 3*10^{16}$.

Table 2 lists the values of constants for the same correlation for local and mean heat transfer coefficients measured at both sides of the baffle plates. For the whole baffle, the average value of $\overline{Nu}$ for air-water system can be given as

$$\overline{Nu} = 9.8 Re_{p/v}^{0.129} \cdot Pr^{0.33} \left(\frac{\mu_w}{\mu_b}\right)^{-0.14} \tag{18}$$

Conclusions

A Positive Tempareture Coefficient Thermister has been devised to serve as a local heat transfer coefficient probe and applied to a standard single-impeller aerated stirred tank to study the variation of heat transfer rates at the cylindrical wall and the surface of the baffle of the vessel with positions and operating variables.

The experimental results show that amount of heat transfer heavily depends on the state of agitation in the non-aerated system. The highest heat transfer coefficient was found at the front side of baffle plate near the impeller and larger values of local heat transfer coefficients were observed at the impeller discharge region. The location of the highest local h shifted upward slightly as a result of aeration. Under flooding conditions, the heat transfer coefficient in the impeller discharge region sharply decreased due to insufficient pumping of the impeller at this state, and a larger heat transfer coefficient was seen at near the free surface.

For different θ locations at the wall surfaces, a higher heat flux was seen near front of the baffle plate (i. e. θ = 86°), and a 5~6% difference was found among the three different θ locations.

For an aerated srirred system the mean value of Nu at the mid-plane for air-water system has been correlated by Eq. (17).

The modified Reynolds number has been introduced here to take into account both aeration and agitation conditions.

Acknowledgment

The authors wish to express thier sincere appreciation for the financial support given by the National Science Council, R. O. C., for this study.

Nomenclature

a	=	exponent on Reynold number	[-]
A	=	surface area of the probe	[m^2]
c	=	coefficient of correlation equation	[-]
d	=	internal diameter of circular conduit	[m]
D	=	diameter of the impeller	[m]
h	=	local heat transfer coefficient	[$W/(m^2 \cdot K)$]
$\bar{h}$	=	mean heat transfer coefficient	[$W/(m^2 \cdot K)$]
H	=	height of non-aeration liquid from bottom of stirred tank	[m]
I_p	=	electrical current through the probe	[A]
k_L	=	thermal conductivity of liquid	[$W/(m \cdot K)$]
N	=	rotational speed of the impeller	[1/s]
P	=	power of impeller	[W]
Pa	=	power consumed by aeration	[W]
P_g	=	power of impeller under aeration	[W]
P_o	=	power of impeller under aeration	[W]
q_{conv}	=	convective heat flow rate	[W]
q_{loss}	=	heat loss of the probe	[W]
Q_g	=	gas flow rate	[m^3/s]
R_1	=	reference resistance	[Ω]
R_2	=	reference resistance	[Ω]
R_3	=	reference resistance	[Ω]
R_f	=	reference resistance	[Ω]
R_p	=	reference of the probe	[Ω]
t	=	time	[s]
T	=	vessel diameter	[m]
T_b	=	back side surface temperature of PTC	[K, °C]
T_f	=	fluid temperature	[K, °C]
T_s	=	front side surface temperature of PTC	[°C]
Ub	=	bulk velocity in circular conduit	[m/s]
V_s	=	superficial gas velocity	[m/s]
V	=	volume of non-aeration liquid	[m^3]
V_2	=	voltage of reference resistance R_2	[V]
V_f	=	voltage of reference resistance R_f	[V]
ω	=	anglular velocity	[rad/s]
Z	=	axial coordinate	[m]

<Greek symbols>

μ	=	viscosity	[Pa·s]
μ_b	=	fluid viscosity at bulk fluid temperature	[Pa·s]
μ_w	=	fluid viscosity at wall temperature	[Pa·s]
ρ	=	fluid density	[kg/m^3]
θ	=	angle (see Figure 5)	[°]
υ	=	kinematic viscosity	[m^2/s]
α	=	thermal diffusuvity	[m^2/s]

<Dimensionless groups>

Nu	=	local Nusselt number	$h \cdot T/k_L$
$\overline{Nu}$	=	mean Nusselt number	$\bar{h} \cdot T/k_L$
Pr	=	Prandtl number	υ/α
Re	=	Reynolds number	$N \cdot D^2/\upsilon$
Red	=	Reynolds number	$d \cdot Ub/\upsilon$
$Re_{p/v}$	=	modified Reynolds number	$(P/V) \cdot T^4 \cdot \rho^2/\mu^3$

Literature Cited

Bourne, J. R., O. Dossenbach and T. Post; "Local and Average Mass and Heat Transfer due to Turbine Impellers," 8th European Congress on Mixing. 199-208 (1985)

Calderbank, P. H. and M. B. Moo-Young; "The Continuous Phase Heat and Mass-Transfer Properties of Dispersions," *Chem. Eng. Sci.*, **16**, 39-54 (1961)

Chiton et al.; "Heat Transfer Coefficient in Agitated Vessels," *Ind. Eng. Chem*, **36** (6), 510 (1994)

Churchill, S. W. and H. H. S. Chu; "Correlating Equations for Laminar and Turburent Free Convection from a Vertical Plate," *Int. J. Heat & Mass Transfer*, **18**, 1323-1331 (1975)

Ede, A. J.; "The Heat Transfer Coefficient for Flow in a Pipe," *Int. J. Heat & Mass Transfer*. **4**, 105-110 (1961)

Fasano, J. B., R. S. Brodkey, and S. J. Haam; "Local Wall Heat Transfer Coefficients Using Surface Calorimeters," 7th European Congress on Mixing, 497-505 (1991)

Haam, S. J. and R. S. Brodkey; "Multiphase Local Heat Transfer in a Mixing Vessel," *AIChE Symposium Series*, **88**, 93-97 (1992)

Karcz, J. and Strek, F.; "Heat Transfer in Mechanically Stirred Gas-Liquid System," 7th European Congress on Mixing, 251-259 (1985)

Kutateladze, S. S., Osnovy Teorii Teploobmena., Mashgiz, Moscow, p145 (1957)

Lan, C. M.; "The Study of Local Heat Transfer in an Aerated Stirred Tank," M.S. Thesis, National Taiwan Uneversity, Taipei, Taiwan (1993)

Loiseau, B. and J. C. Charpentier; "Some Hydrodynamics and Power Input Data in Mechanically Agitated Gas-Liquid Contactors," *AIChE J*, **23** 931-935 (1977)

Man K. L.; "A Study of Local Heat Transfer Coefficient in Mechanically Agitated Gas-Liquid Vessels," 5th European Congress on Mixing. 221-231 (1985)

Michel, B. J. and S. A. Miller; "Power Requirement of Gas-Liquid Agitated Systems," *AIChE J.* **8**, 262-266 (1962)

Stieff, A.; "Power Comsumption and Heat Transfer in Stirred Gas/Liquid/Solid System," 5th European Congress on Mixing. 209-219 (1985)